Sensors and Materials, Vol. 14, No. 4 (2002) 199–208
MYU Tokyo

S & M 0482

Real-Time Microchip Polymerase-Chain-Reaction System

Yu-Cheng Lin, Min Li, Ming-Ta Chung, Ching-Yi Wu[1] and Kung-Chia Young*[2]

Department of Engineering Science, [2]Department of Medical Technology,
National Cheng Kung University, Tainan, Taiwan
[1]Electronics Research and Service Organization,
Industrial Technology Research Institute, Hsinchu, Taiwan

(Received October 20, 2001; accepted January 14, 2002)

Key words: PCR chip, MEMS, HCV, Real-time detection

A real-time micro-polymerase chain reaction (μ-PCR) system was developed to monitor the amplification of the complementary DNA (cDNA) molecules of the hepatitis C virus (HCV). This system uses SYBR Green I dye as a fluorescent probe for real-time detection in the PCR process. The μ-PCR chip was fabricated on a silicon wafer and Pyrex glass using photolithography, wet etching, and anodic bonding. Compared to the polypropylene tube used in conventional PCR equipment, the silicon reaction well, which has a high thermal conductivity, can improve the temperature uniformity of the sample and the desired temperature can be attained more rapidly. The closed-loop thermal cycling system consists of power supplies, a thermal generator, a computer-controlled PID controller, a data acquisition subsystem, and a fluorescent microscope. Fluorescence was monitored at the end of the 72°C step of the PCR cycle at five-cycle intervals. This μ-PCR system enables *in situ* detection and achieves 35 thermal cycles in 26 min. Different initial concentrations of HCV cDNA were used and good performance of this μ-PCR system was verified. Using this real-time μ-PCR system, it is possible to achieve DNA amplification with real-time detection within 26 min.

1. Introduction

After the polymerase chain reaction (PCR) method was first proposed by Saiki *et al.*[1] in 1985, it has been widely employed to amplify DNA. It has been extensively used in

*Corresponding author, e-mail address: yuclin@mail.ncku.edu.tw

biotechnology, diagnosis of diseases, and genetic engineering. A number of researchers have attempted to improve the efficiency of PCR, particularly by increasing the reaction speed and analysis of PCR kinetics. Following Northrup and coworker's successful amplification of DNA in microfabricated reaction chambers,[2,3] it became possible to miniaturize MEMS-based PCR chambers and shorten the thermal cycle time. These microfabricated PCR devices have the advantages of smaller sample volume required, quicker thermal cycling and lower cost. Cheng *et al.* used silicon-glass chips to investigate sample preparation and amplification on a microchip.[4] Integration of PCR amplification and capillary electrophoresis established the possibility of high-speed DNA analysis using MEMS-based devices. A β-globin target was used as a model in that study.[5] A thermocapillary pump, thermal-cycling chambers, gel electrophoresis channels and a DNA detector were integrated to improve DNA analysis speed, portability and cost. Chip elements were used for fast thermocycling.[6] A thin-film heater was fabricated in a micro-reaction chamber. By finite-element analysis and experimental measurements, the heating and cooling rates were determined to be 80 and 40 K/s, respectively.[7] A microfabricated built-in thin-film heater was used to generate fast thermal response during heating. It was determined that micromachined thin-film heaters in micro-PCR chambers have an extremely fast thermal response, although they may possibly introduce thermal heterogeneities.[8] The capillary nanoliter-scale reactors, which are heated and cooled by air, coupled to electrophoresis chips were designed.[9] A continuous-flow PCR was designed on a chip using three different temperature zones.[10] Recently, a μ-PCR chip for amplification of HCV cDNA was successfully fabricated in our laboratory.[11,12] This instrument consists of power supplies, a thermal generator, a computer-controlled PID controller, and a data acquisition subsystem. A reaction of 30 cycles in the present μ-PCR chip was achieved in 30 min. This device can amplify DNA in a relatively short time but it cannot detect the DNA amplification *in situ*.

Higuchi *et al.*[13] constructed an intercalator-based system for detecting PCR products as they accumulate in real time. The amplified double-stranded DNA molecules bind the intercalator ethidium bromide in each amplification reaction, resulting in an increase in fluorescence. The 5' nuclease PCR technique enables real-time detection of specific amplicons.[14] Lee *et al.*[15] developed fluorogenic probes and improved the real-time method for detecting specific amplification products. Ibrahim *et al.* of Northrup's group[16] distinguished single-base differences in viral and human genes using the 5' nuclease PCR technique and capillary electrophoresis carried out in a miniature analytical thermal cycling instrument. Furthermore, PCR amplification and fluorescence detection were carried out by Northrup's group using a notebook thermal cycler.[17] PCR was accomplished in 25 or 100 μL polypropylene tubes. The 5' nuclease assay enables the detection of target-specific products; however, the probe used in this assay must be custom-synthesized. A study on the feasibility of integrating optical fibers and a photodiode into the micro-PCR reaction chamber for *in situ* detection of fluorescence emission has been carried out.[18] However, an actual PCR process has not been demonstrated in this system.

A μ-PCR system capable of real-time detection is designed and developed herein. SYBR Green I dye (Biowhittaker Molecular Applications, USA) is used for the fluorescent probe in the present investigation. The influence of different concentrations of SYBR Green I dye on the PCR process is studied and discussed in this paper.

2. Experiment

2.1 *Design and fabrication of μ-PCR chips*

Micro-PCR chips were designed to fabricate a reaction well onto a silicon wafer. Hole-drilled Pyrex glass dies are anodically bonded to the etched and diced silicon pieces to form reaction channels for PCR. The μ-PCR chip has a serpentine reaction channel with two holes for easy loading and unloading, and a detection area for real-time fluorescence signal monitoring, as shown in Fig. 1. Capillary force draws the sample into the serpentine channel in the loading process. If further analysis is necessary, compressed air is introduced into one hole to expel the sample for unloading. The serpentine channel is 1000 μm wide and 150 μm deep, with a total length of 19 cm, thus having a 25 μl reaction volume. A 2×4 mm^2 detection area was incorporated in the channel for easy detection. In this design, 25 μl of a sample can be easily drawn from the reaction channel. The use of a 25 μl reaction volume is necessary for further amplicon verification using slab gel electrophoresis. The μ-PCR chip can be further improved without changing the size of the detection area, channel width or depth, by shortening the loading and air outlet channels to 5 mm, which results in a small sample volume of as low as 2.5 μl. The Pyrex glass has two electrochemically drilled 1 mm holes: one for manual loading of the 145 base-pair (bp) HCV cDNA samples, and the other for removal of the sample after amplification if further analysis is needed. The etched silicon wafer undergoes thermal oxidation by which a 0.3-μm-thick oxide layer regrows, which prevents the DNA sample from reacting with the bare silicon surface.[19] After oxidation, the silicon wafers are diced and then anodically bonded to Pyrex glass pieces to form μ-PCR chips.

2.2 *Rapid thermal cycle system*

The rapid thermal cycle system consists of three subsystems: a computer-controlled PID controller, a power unit and a data acquisition subsystem. The schematic of the structure of the entire system is shown in Fig. 2. The controller consists of a computer and

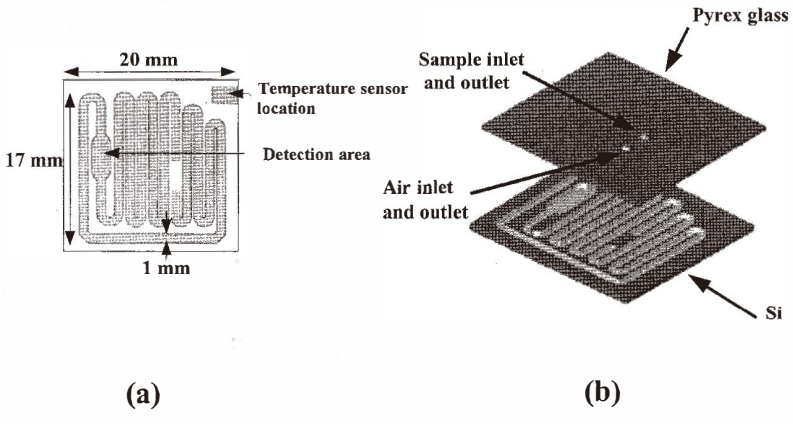

Fig. 1. Schematics of the m-PCR chip: (a) top view and (b) enlarged view.

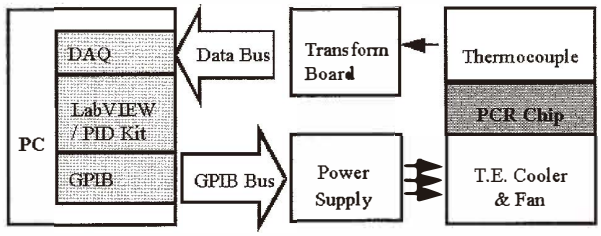

Fig. 2. Structure of the entire system.

LabVIEW 6.0 with a PID kit (National Instruments, USA). The power unit includes two-channel power supply units and a thermal generator. The thermal generator and the data acquisition subsystem are connected to the PID control unit via a GPIB interface to form a closed-loop system. The thermal unit uses one thermoelectric (TE) cooler that functions as a thermal generator or a heat sink when the electrical power polarity is reversed. Each cycle consists of three steps: denaturation at 94°C, primer annealing at 55°C, and primer extension at 72°C. The holding time varies from 7 to 10 s at different steps. The approximate heating rates from 55 to 72°C and from 72 to 94°C are 4.4°C/s and 2.75°C/s, respectively. The cooling rate from 94°C to 55°C is 8.3°C/s. The thermal transition rates are relatively slow for a silicon device due to the heating and cooling capabilities of the TE cooler. The maximum temperature deviation for this rapid thermal cycle system is 0.3°C at the 94°C step. Figure 3 shows the detailed temperature profile of the μ-PCR chip.

2.3 *Real-time detection system*

Figure 4 shows a schematic of the setup of the real-time fluorescence detection system. The excitation light is generated using a mercury lamp, filtered by a 460–490 nm band-pass filter and focused on the detection spot of the μ-PCR chip through an optical microscope (BX60, Olympus, Japan). The excitation light is controlled to excite the amplicon at five-PCR-cycle intervals using a computer-controlled shutter. The fluorescence induced from the SYBR Green I dye bound to the double-stranded DNA is filtered using a 515 nm high-pass filter and detected through an optical microscope using a photomultiplier tube (R928, Hamamatsu, Japan). The signal processing and driving voltage control for opening the shutter are operated using LabVIEW 6.0 software.

2.4 *DNA detection with SYBR Green I dye*

The SYBR Green I dye, a double-stranded-DNA-binding dye, is used in this study. Unbound molecules of the dye exhibit background fluorescence. However, when the dye binds to the DNA, the intensity of fluorescence is greatly enhanced.

At the denaturation step of amplification, the reaction mixture contains single-stranded DNA, the primers and the dye. The unbound dye molecules show weak fluorescence under light excitation, producing a minimal background fluorescence signal. When primers are annealed to the DNA template, a portion of the dye molecules can bind to the double-stranded DNA. DNA binding results in a significant increase in the intensity of the

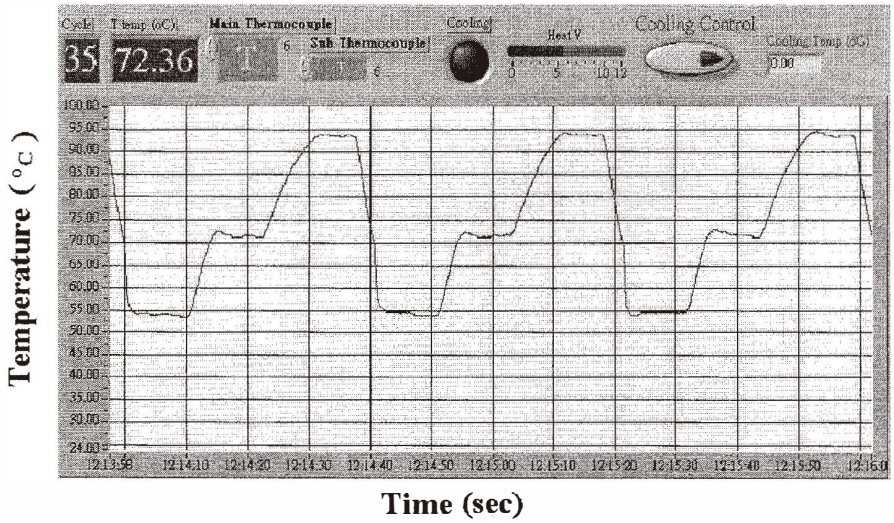

Fig. 3. Actual thermal cycle profiles of the μ-PCR system for HCV from LabVIEW package.

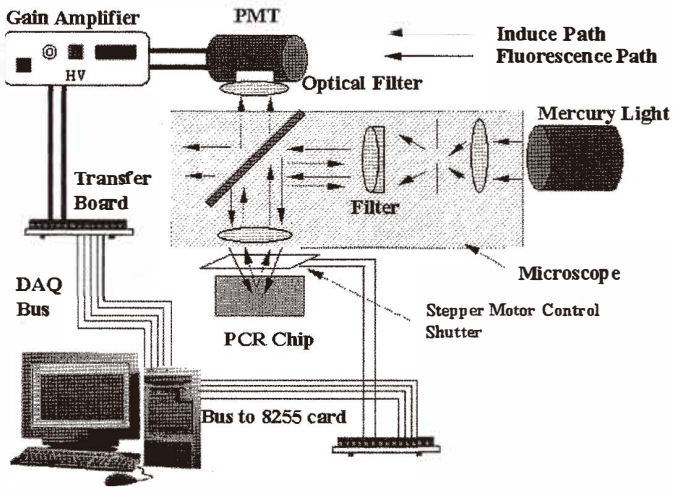

Fig. 4. Schematic of the real-time detection system.

fluorescence signal of the SYBR Green I dye molecules upon excitation. During elongation, the number of dye molecules that continually bind to the newly synthesized DNA increases. An increase in fluorescence is observed in real time while the reaction is monitored continuously. Upon denaturation of the DNA for the next heating cycle, the dye

molecules are released and the fluorescence signal decreases. Fluorescence at the end of the elongation step is measured every five PCR cycles to monitor the increase in the amount of amplified DNA amplicon.

3. Results and Discussion

Many dyes can be used in signal detection, for example, ethidium bromide. However, the fluorescence of unbound ethidium bromide may influence the detection results. The advantage of using the SYBR Green I dye is that unbound SYBR Green I dye molecules have weak fluorescence and exhibit a very low background intensity under excitation. The signals of SYBR Green I dye at different concentrations before binding to the DNA samples were below 0.8 V with a 0.1 V noise signal. After offsetting the signal by deducting the 0.8 V background signal to designate 0.8 V as the new origin, the meaningful signal must be greater than 1.1 V (1.1 V being the background signal plus 0.3 V (S/N = 3)). High concentrations of the matrix chemicals along with SYBR Green I dye may inhibit the DNA amplification. To obtain the optimum concentration of SYBR Green I dye for PCR amplification, the dye was diluted from its initial stock concentration to four concentrations, 1000×, 5000×, 10000× and 50000×, and mixed with individual HCV cDNA samples. The mixing ratio of 145-bp HCV cDNA to SYBR Green I dye was 50 to 1. The mixtures were loaded into the commercial PCR units GeneAmp 2400 (Perkin-Elmer, USA), and amplified through 35 identical PCR cycles. The amplicons were analyzed using slab gel electrophoresis with an appropriate DNA marker. Figure 5 shows the electrophoresis result for the PCR products. The weak band corresponds to HCV cDNA amplified with the

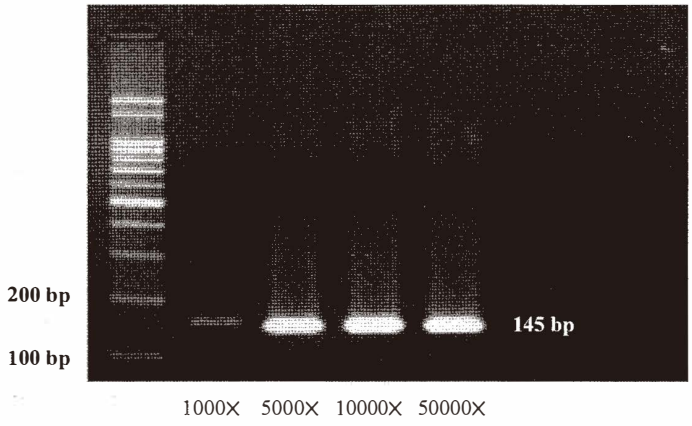

Fig. 5. Electrophoresis results for amplification products with different concentrations of the SYBR Green I dye bound to the HCV amplicon. The amplicons were analyzed using slab gel electrophoresis with simultaneous separation of a DNA marker (100 bp ET Mark, Bertec, Taiwan). The DNA marker consists of eight fragments that range in size from 100 to 1000 bp in 100 increments, plus additional fragments of 1500 and 2000 bp.

SYBR Green I dye at the initial diluted concentration of 1000×. The appropriate pH for the PCR process is about 7.4, which is weakly alkaline. The SYBR Green I dye is dissolved in dimethyl sulfoxide (DMSO) solvent, which is an acid with a pH of 3–4. Increasing the amount of DMSO will change the mixture of the DNA sample and SYBR Green I dye from alkaline to acid, which will inhibit the PCR process. The signal intensity in the slab gel electrophoresis remained unchanged whether SYBR Green I dye was diluted 5000×, 10000× or 50000×. Therefore, the concentration of SYBR Green I dye of 5000× was used in further experiments.

The mixture of HCV cDNA and 5000×-diluted SYBR Green I dye was portioned into eight aliquot samples which were then loaded into the GeneAmp 2400 for analyses using different numbers of thermal cycle amplifications. For comparison, the thermal cycle numbers were set from zero to 35 cycles at five-cycle increments. The complete thermal cycle consisted of denaturation for 2 min, amplification for the desired number of cycles, and a final extension for 10 min. Each amplification cycle consisted of three steps, namely, denaturation at 94°C for 1 min, primer annealing at 55°C for 1.5 min, and primer extension at 72°C for 1.5 min. The total thermal cycling time was 3.2 h. The amplicons were taken out at the desired thermal cycle number, loaded into the μ-PCR chips and maintained at 72°C for signal detection. The fluorescence intensities at different thermal cycles are plotted in Fig. 6. The optimum detection point is at the end of the extension process which, in this case, was 72°C. However, it was found that if no denaturation occurs, the fluorescence signal intensity increases at lower temperatures. The main purpose of loading the amplicons into μ-PCR chips is to establish the same parameters for signal detection, thereby improving the reliability as a reference curve. The fluorescence intensities

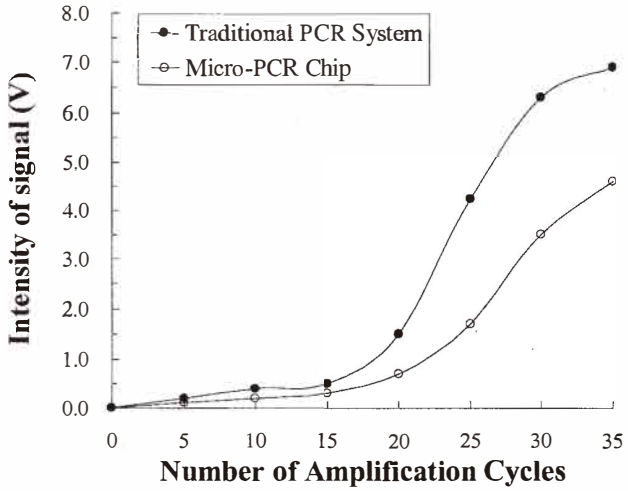

Fig. 6. Amplification of HCV cDNA using the conventional PCR (GeneAmp 2400) system and the m-PCR system. The background signal has been deducted from the signals.

increase slightly in the initial cycles of PCR, and then increase significantly at the start of cycle 20. The signal becomes detectable at cycle 15, which is referred to as the threshold point in this measurement.

The same sample mixture of HCV cDNA and SYBR Green I dye was loaded and amplified in the μ-PCR system. Measurement of fluorescence intensity was performed at the end of the elongation step every five PCR cycles to monitor the increase in the amount of amplified DNA amplicon. The complete thermal cycle consists of denaturation for 30 s, amplification for the desired number of cycles, and a final extension for 30 s. Each amplification cycle consists of three steps, namely, denaturation at 94°C for 7 s, primer annealing at 55°C for 10 s, and primer extension at 72°C for 8 s. The total thermal cycling time is 26 min. The fluorescent intensity significantly increases at cycle 25 in the μ-PCR system, as shown in Fig. 6. As compared to the conventional PCR device, the μ-PCR system carries out five more cycles to achieve comparable signals, which takes approximately 4 more minutes, as shown in Fig. 6. The μ-PCR system requires 26 min to complete the 35 thermal cycles. GeneAmp 2400 requires 3.2 h for 35 cycles, and 40 min for gel electrophoresis as well as the time for sample transport. The μ-PCR system can perform the PCR process with *in situ* detection much faster than GeneAmp 2400. The thermal cycling profile of the μ-PCR system is currently not optimized, so the threshold points are not reached at the same cycle number. Using the data in Fig. 6 for comparison of the signal strength between the amplicons obtained using the conventional equipment and those from the μ-PCR system, it is found that 5 to 10 additional cycles are required for the μ-PCR system to reach the same signal level of the amplicons in GeneAmp 2400 (about 4 to 7 min).

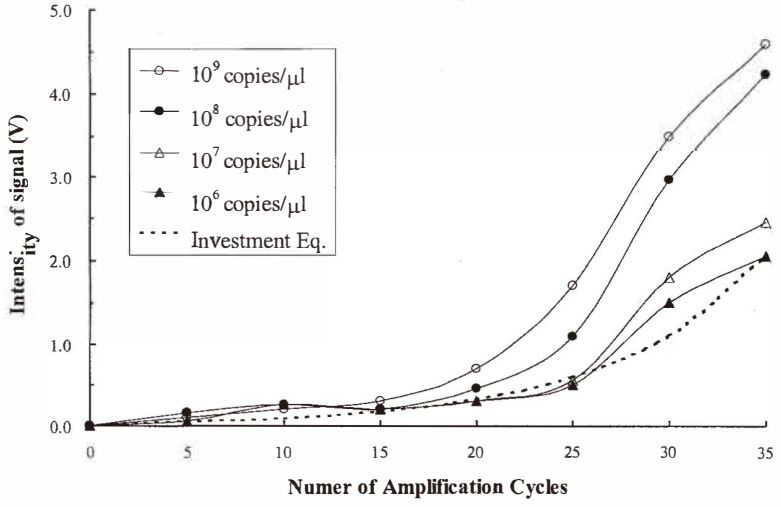

Fig. 7. Amplification of the HCV cDNA at different initial concentrations using the μ-PCR system. The background signal has been deducted from the signals.

Different initial concentrations of HCV cDNA were used to verify the performance of the real-time μ-PCR system. The concentrations were 10^6, 10^7, 10^8 and 10^9 copies/μl. The same thermal cycling setup as described above for the μ-PCR system was used to perform the amplification and signal detection. Figure 7 shows the real-time-detected fluorescence intensities for different initial DNA concentrations during the amplification process. Lower initial DNA concentrations exhibited higher threshold cycle and lower fluorescence intensity during the amplification process. The investment equation for quantitative PCR is

$$Y = X(1 + E)^n, \tag{1}$$

where Y is the PCR product yield, X the input target amount, E the efficiency, and n the cycle number. Based on the PCR amplification data using an initial concentration of 10^6 copies/μl and eq. (1), the efficiency E obtained from the curve shown in Fig. 7 is 0.13. The limit of detection, defined as S/N > 3, must therefore be reached at 1.1 V, as mentioned above. Using an HCV cDNA initial concentration of 10^6 copies/μl, cycle number 25 (where 1.1 V is detected), and efficiency E of 0.13, the limit of detection is 35 pM HCV cDNA.

4. Conclusions

The μ-PCR chip was equipped with a TE cooler and a closed-loop temperature control system in order to perform the necessary temperature cycles for PCR amplification. The reaction well was fabricated onto silicon, which has a high thermal conductivity. The device can reach the desired temperature rapidly and improve the temperature uniformity of the sample. SYBR Green I dye acts as a fluorescent probe when bound to the DNA double helix and signals real-time detection during the PCR process.

Several different dilution concentrations of SYBR Green I dye were tested with DNA amplification. The use of 5000× concentration, compared to 1000×, resulted in better signal intensity as well as less interference. However, a quantitative study of dilutions higher than 5000× may be useful for further investigation. During the PCR process, the signal was detected at the end of the elongation step every five PCR cycles to monitor the increase in the amount of amplified DNA amplicon. Different initial concentrations of HCV cDNA were used and good performance of this μ-PCR system was verified.

The real-time detection system with the μ-PCR chip was successfully established in the present study. Compared with conventional PCR equipment, this real-time μ-PCR system requires only a very small amount of sample, and enables a rapid thermal cycling process and real-time detection of DNA amplification. This real-time μ-PCR system may benefit potential applications in DNA amplification.

References

1 R. K. Saiki, S. Scharf, F. Faloona, K. B. Mullis, G. T. Horn, H. A. Erlich and N. Arnheim: Science **230** (1985) 1350.
2 M. A. Northrup, M. T. Ching, R. M. White and R. T. Watson: Proceedings of the 7th International Conference on Solid State Sensors and Actuators (Transducers'93) 1993 (Yokohama, Japan, June 1993) p. 924.
3 M. A. Northrup, C. Gonzalez, D. Hadley, R. F. Hills, P. Landre, S. Lehew, R. Saiki, J. J. Sninsky, R. Watson and R. Watson Jr.: Proceedings of the 8th International Conference on Solid-State Sensors and Actuators, and Eurosensors IX 1995 (Stockholm, Sweden, June 1995) p. 764.
4 J. Cheng, M. A. Shoffner, G. E. Hvichia, L. J. Kricka and P. Wilding: Nucleic Acids Res. **24** (1996) 380.
5 A. T. Woolley, D. Hadley, P. Landre, A. J. deMeHo, R. A. Mathies and M. A. Northrup: Anal. Chem. **68** (1996) 4081.
6 M. A. Burns, C. H. Mastrangelo, T. S. Sammarco, F. P. Man, J. R.Webster, B. N. Johnson, B. Foerster, D. Jones, Y. Fields, A. R. Kaiser and D. T. Burke: Proc. Natl. Acad. Sci. U. S. A. **93** (1996) p. 5556.
7 S. Poser, T. Schulz, U. Dillner, V. Baier, J. M. Kohler, D. Schimkat, G. Mayer and A. Siebert: Sensors and Actuators A **62** (1997) 672.
8 M. A. Northrup, B. Benett, D. Hadley, P. Landre, S. Lehew, J. Richards and P. Stratton: Analytical Chemistry **70** (1998) 918.
9 S. A. Soper, S. M. Ford, Y. Xu, S. Qi, S. McWhorter, S. Lassiter, D. Patterson and R. C. Bruch: Journal of Chromatography A **853** (1999) 107.
10 M. U. Kopp, A. J. de Mello and A. Manz: Science **280** (1998) 1046.
11 Y. C. Lin, C. C. Yang and M. Y. Huang: Sensors and Actuators B **71** (2000) 127.
12 Y. C. Lin, M. Y. Huang, K. C. Young, T. T. Chang and C. Y. Wu: Sensors and Actuators B **71** (2000) 2.
13 R. Higuchi, C. Fockler, G. Dollinger and R. Watson: Kinetic PCR Biotechnology **11** (1993) 1026.
14 P. M. Holland, R. D. Abramson, R.Watson and D. H. Gelfand: Proceedings of National Academy of Sciences USA **88** (1991) p. 7276.
15 L. G. Lee, C. R. Connell and W. Bloch: Nucleic Acids Research **21** (1993) 3761.
16 M. S. Ibrahim, R. S. Lofts, P. B. Jahrling, E. A. Henchal, V. W. Weedn, M. A. Northrup and P. Belgrader: Analytical Chemistry **70** (1998) 2013.
17 P. Belgrader, S. Young, B. Yuan, M. Primeau, L. A. Christel, F. Pourahmadi and M. A. Northrup: Analytical Chemistry **73** (2001) 286.
18 C. G. J. Schabmueller, J. R. Pollard, A. G. R. Evans, J. S. Wilkinson, G. Ensell and A. Brunnschweiler: J. Micromech. Microeng. **11** (2001) 329.
19 M. A. Shoffner, J. Cheng, G. E. Hvichia, L. J. Kricka and P. Wilding: Nucleic Acids Res. **24** (1996) 375.